Geometrical Modeling of Wideband MIMO Channels
Modelado de Canales MIMO de Banda Ancha por Métodos Geométricos

Alberto Alcocer Ochoa[1], Ramón Parra Michel[2] and Valeri Ya. Kontorovitch[3]

[1,3] CINVESTAV del IPN, Av. IPN 2508, Col. San Pedro Zacatenco, G. A. Madero, C. P. 07360, México D. F., México.
[2] CINVESTAV del IPN, campus Guadalajara. Av. Científica 1145, Col. El Bajío, C. P. 45010, Jalisco, México.
`aalcocer@cinvestav.mx`[1], `rparra@gdl.cinvestav.mx`[2], `valeri@cinvestav.mx`[3]

Abstract

In this paper it is shown a geometrically–based (GB) channel model that is proposed for the macro–, micro– and picocell environments. It is assumed that the local and dominant scatters' positions are given in a uniform way. The model includes some simplifications by the use of the mean values of the scatters' positions random variables (RV) as well as by the use of an asymptotic approach, i. e., it is assumed that the distance from the mobile to the base station is larger than the scatters–region's dimensions. The main idea is to find a closed form for the angle of arrival (AoA) and delay probability density functions (PDF) in order to evaluate the covariation matrix of the channel.
Keywords: Geometrical Models; Wideband MIMO Channels; Macrocell, Microcell and Picocell Environments.

Resumen

En este artículo se muestra un modelo de canal basado en geometría, para los ambientes de propagación macrocelda, microcelda y picocelda. Se asume que la posición de los dispersores locales y dominantes está dada de manera uniforme en cada región. El modelo incluye algunas simplificaciones mediante el uso de los valores promedio de las posiciones de los dispersores (vistas como variables aleatorias) en cada región, así como de un caso asintótico, i. e., se asume que la distancia del móvil a la estación base es mucho mayor que las dimensiones de la región donde yacen los dispersores. La idea principal detrás de este artículo es hallar una forma cerrada para función de densidad de probabilidad del ángulo de arribo y del tiempo de retardo para con ello evaluar la matriz de covarianza del canal MIMO.
Palabras Claves: Ambientes Macrocelda, Microcelda y Picocelda; Canales MIMO de Banda Ancha; Modelos Geométricos.

1 Introduction

The propagation models, which have been developed to date in order to simulate the radio channels, have evolved according to the needs of the mobile communications industry. Consequently, there is currently a demand for new models that will provide the required spatial and temporal information needed to study the emerging fourth generation of communications systems.

Multiple–Input Multiple–Output (MIMO) channels are commonly called vectorial channels as for each transmitter–receiver antenna pairs, there is established a channel. In this context, for every single channel we are trying to model the spatio–temporal channel statistics with the help of a geometrical model.

The spatio–temporal models can be generally classified into two groups [Molisch04, Piechocki01]: deterministic and stochastic. With the deterministic models, the channel impulse response is obtained by tracing the reflected, diffracted and scattered rays, within the help of databases that provide information about the size and location of the physical structures in addition to the electromagnetic properties of their materials. Deterministic models have the advantage of providing the ability to generate accurate site specific and easily reproducible information. Stochastic models, on the other hand, describe characteristics of the radio channel by means of the joint Probability Density Function (PDF). Statistical parameters employed in such models are usually estimated from extensive measurement campaigns or

inferred form geometrical assumptions. Stochastic models usually need less information than deterministic ones, and they produce more general results, as many repetitions are considered.

The axioms corresponding to a priori properties of the channel that is modeled using a geometric approach must represent realistic wave propagation. In a geometric channel model, the spatial pattern of scatters is defined by a set of logical relationships satisfying a set of axioms (wave propagation obeying diffraction, reflection and scattering laws), which are in turn interpreted as true statements about the model. Subsequently, one can safely infer the process behavior from the model's one if and only if the model closely corresponds to the process. However, the spatial pattern of the scatters and their density in the scattering areas in the existing geometric channel models has been defined with a certain level of ambiguity.

Most of the existing geometric channel models take into account only the local scattering cluster [Chen04], which is always located around the mobile unit with few available models defining the shape and distribution of far clusters. The geometrical channel models are well suited for simulations that require a complete model of the wireless channel, due to its ray–tracing nature. However, the shape and size of the spatial scatters' density function required to achieve a reliable simulation of the propagation phenomenon is subject to debate.

The wireless channel is typically a multipath channel due to the natural and man–made objects, which are situated between the base station (BS) and the mobile station (MS). At the receiver, the waves arriving from different directions are combined vectorially to produce a composite received signal. If only one discrete scatter is present, a closed expression can be easily found from the signal at the receiver by using fundamental wave propagation and scattering laws. However, if many objects are present, things become much more complicated, since the interaction between different objects must be accounted for. Consequently, a more complex model would result if multiple bounces are to be accurately modeled.

The main idea of this paper is to find the Time Delay or Time of Arrival (ToA) and the Angle of Arrival (AoA) PDFs. Analytical analysis using geometrical MIMO models, from our point of view, is an appropriated tool in order to investigate the channel covariation matrix. It is needed to use a method capable to give us simple analytical expressions.

The paper is organized as follows: on section II it is described the GB channel models for the macro–, micro– and picocell environments, the geometrical relationships between the delay and AoA as functions of the related parameters are obtained in section III, as well as the scatters' position PDF. In section IV the delay and AoA PDF are derived taking into account several approaches, and some numerical results are shown and finally, section V gives some comments and concluding remarks.

2 Geometrical Description of the Model

For any geometrical–based (GB) channel model, the signal statistics depends on the position of the BS, the MS and the geometrical distribution of the scatters around the BS and the MS. In order to simplify the derivation of the expression for the radio channel characteristics, two important assumptions are made within the GB channel model. Firstly, that the signal undergoes by two reflections at most as it travels from the BS to the MS [Molisch04], and secondly, that all scatters are confined within a scattering region.

It is worth to mention here that the scenarios considered are modeled in two different ways: for the macrocell environment it is needed to consider what is shown in Fig. 1, as it is mentioned in [Ertel99, Piechocki01]. For the picocell environment it is needed to consider what it is shown in Fig. 2, as it is mentioned in [Ertel98, Chizhik02]. We should mention here that, as far as we know, there is not any criterion to follow in order to classify the microcell environment, thus it can be included in the model depicted at Fig. 1 or in the one at Fig. 2.

The assumed geometry for the model is depicted for the picocell environment at Fig. 2. The model is appropriate for the microcell environment as well [Ertel99], where the antenna heights are relatively low. With low antenna heights, the BS may also receive multipath reflections from locations near the BS as well as around the MS. The elliptical model has the physical interpretation that only multipath components with time delay smaller than the specified maximum time delay are considered. Ignoring path with longer delays may be justified, since such signals components will experience greater path loss and hence will have relatively low power compared to those with shorter delays. Therefore, provided that the maximum delay is sufficiently large, nearly all of the power of the multipath signals of a physical channel will be accounted for by the model.

Alberto Alcocer Ochoa, Ramón Parra Michel and Valeri Ya. Kontorovitch

In the models in Fig. 1 and Fig. 2, it is distinguished two kinds of scatters: the local scatters, which are confined into a circular region surrounding the MS (BS), and the dominant scatters, which are in a circular ring around the MS (BS) in Fig. 1, and in an elliptical region as depicted in Fig. 2. We included here a dominant scatters region around the BS for generality as we consider this model for the microcell environment as well, where it is necessary to do. The dominant scatters contribute to spread the power azimuth spectra (PAS) and the power delay profile (PDP) more than the local ones and due to this phenomenon is why we include them in the analysis.
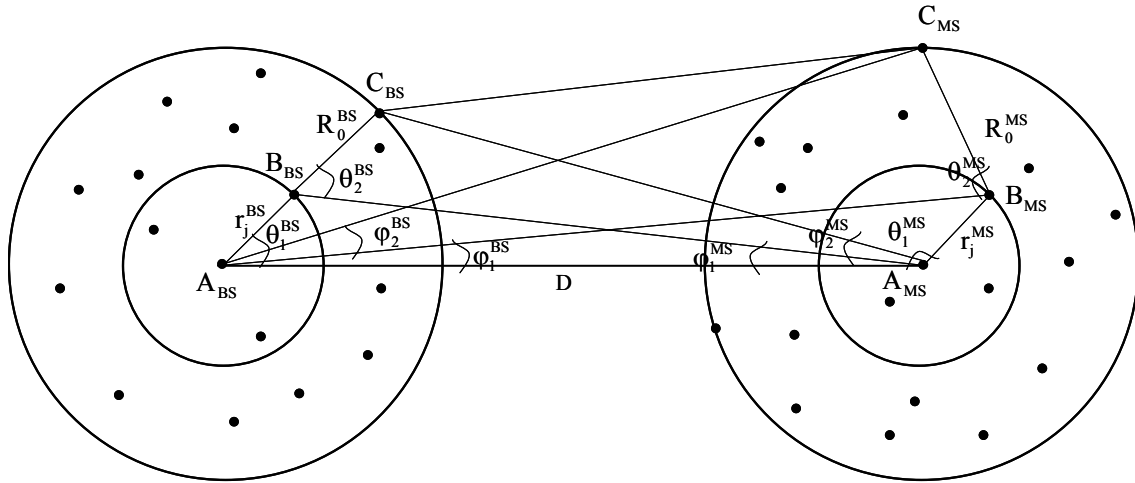

Fig. 1. The macrocell and microcell environment scenarios.

The model assumes a uniform distribution of the local and dominant scatters' positions at the surrounding of the MS and the BS. The channel properties are derived from the scatters' positions by the application of fundamental electromagnetic waves propagation. The signals received at the MS are plane waves which propagate on the horizontal plane (i. e., we are considering a two–dimensional model), and the scatters are treated as omni–directional re–radiating elements.

We tried to describe in a stochastic way, the delay and AoA to the antenna array at the MS (BS), using uniform scatters positions' PDF at the presented regions at the surrounding of the MS (BS). Then, let us consider the scenarios depicted at Fig. 1 and Fig. 2.
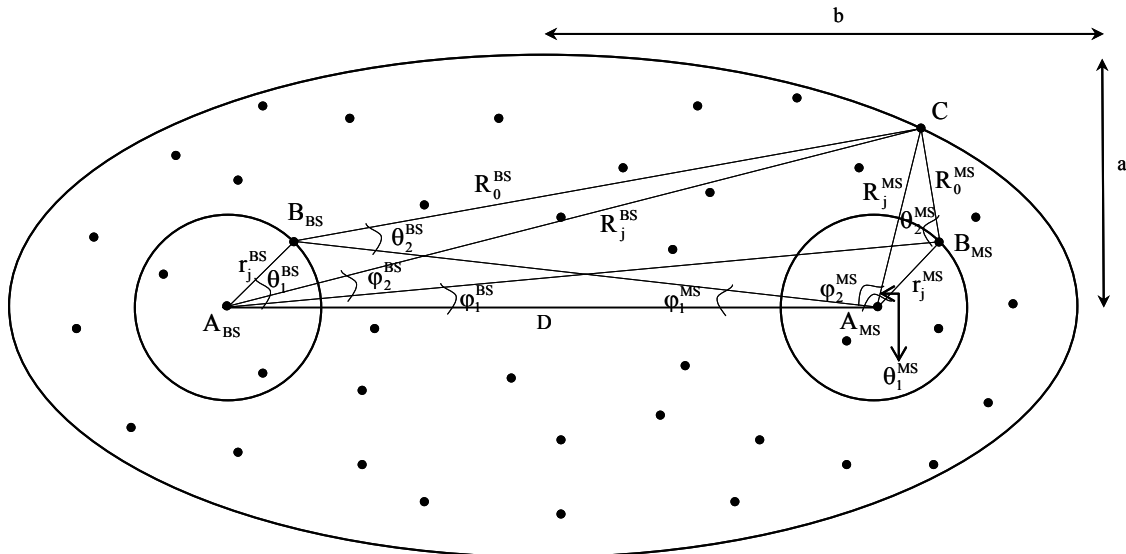

Fig. 2. The microcell and picocell environment scenarios.

328

Before we continue, let us define:

$A_{MS(BS)}$ The MS (BS) position.

$B_{MS(BS)}$ The position of the local scatter at the surrounding of the MS (BS).

$C_{MS(BS)}$ The position of the dominant scatter at the surrounding of the MS (BS), or C in Fig. 2 where it is the common dominant scatter position.

Additionally we define:

D The distance between the MS and the BS.

$D_{MS(BS)}$ The distance between the MS (BS) to the local scatter at the surrounding of the BS (MS).

$R_{MS(BS)min}$ The radii of the circular region where the local scatters lie in.

$R_{MS(BS)max}$ The radii of the circular region where the dominant scatters lie in. This definition is used in the macrocell environment only (see Fig. 1).

$r_j^{MS(BS)}$ A random variable (RV) which denotes the position of the local scatter referred to the MS (BS).

$R_j^{MS(BS)}$ A RV which denotes the position of the dominant scatter to the MS (BS).

$R_0^{MS(BS)}$ A RV which denotes the distance between the local and dominant scatters, referred to the MS (BS).

$\theta_1^{MS(BS)}$ Is the angle defined by $B_{MS(BS)} - A_{MS(BS)} - A_{BS(MS)}$.

$\theta_2^{MS(BS)}$ Is the angle defined by $C_{MS(BS)} - B_{MS(BS)} - A_{BS(MS)}$.

$\varphi_1^{MS(BS)}$ Is the angle defined by $B_{BS(MS)} - A_{MS(BS)} - A_{BS(MS)}$.

$\varphi_2^{MS(BS)}$ Is the angle defined by $C_{BS(MS)} - A_{MS(BS)} - B_{BS(MS)}$.

Some of the definitions given above are shown at Fig. 1. We will consider only the downlink, as the uplink is also considered by exchanging the sub–indexes BS by MS and viceversa. In the model depicted at Fig. 2, we had assumed that the BS and the MS are at the foci of the ellipse as it is done in [Ertel99, Oestges03]. The results derived here apply to the ensemble or randomly located local and dominant scatters and do not precise the functional form of the angle of departure (AoD) PDF. We did not consider a specific number of scatters present.

It have to be mentioned that if the angular dimension of the scatters is much more large than the antenna aperture, then all the trajectories form all antennas are illuminating the k–th cluster of scatters practically at the same angle. Though, each trajectory presented at Fig. 1 and Fig. 2 represents the component Hkm,n(t,τ,θ) of the MIMO channel impulse response function for the k–th scatter between the m–th and n–th antennas. Otherwise if the assumptions of those homogeneous conditions for reflection (refraction) for each scatter are not valid, and one would have to take into account all possible combinations for antennas at the BS and the MS. This is a deadlocked approach if the number of antennas is large.

3 RV Relationships and the PDFs of the Scatters Positions

The relationships between the AoD and the AoA are given by means of geometrical consideration [Laurila98], some of them are:

$$\varphi_1^{MS(BS)} = \text{arctg}\left(\frac{r_j^{BS(MS)} \sin(\theta_1^{BS(MS)})}{D - r_j^{BS(MS)} \cos(\theta_1^{BS(MS)})}\right), \tag{1}$$

$$\varphi_2^{MS(BS)} = \text{arctg}\left(\frac{R_0^{BS(MS)} \sin(\theta_2^{MS(BS)})}{D_{MS(BS)} - R_0^{BS(MS)} \cos(\theta_2^{MS(BS)})}\right) \tag{2}$$

The PDFs for the local scatters' position for every scenario are given by:

$$W_{r_j^{MS(BS)}}(r_j^{MS(BS)}) = \frac{2r_j^{MS(BS)}}{R^2_{MS(BS)\min}}, \quad 0 \le r_j^{MS(BS)} \le R_{MS(BS)\min}, \tag{3}$$

$$W_{R_j^{MS(BS)}}(R_j^{MS(BS)}) = \frac{2R_j^{MS(BS)}}{R^2_{MS(BS)\max} - R^2_{MS(BS)\min}}, \quad R_{MS(BS)\min} \le R_j^{MS(BS)} \le R_{MS(BS)\max}. \tag{4}$$

From the development of those distributions in [Kontorovitch99], it is shown that the azimuth angle for radiation of the (MS) BS does not change the functional form of (3) and (4). For the microcell environment case, the dominant scatters PDF is given in [Alcocer05a] by:

$$W_R(R) = \frac{2abR}{ab - R^2_{MS} - R^2_{BS}}, \quad R \in \Omega, R \notin (\Omega_{MS} \cup \Omega_{BS}), \tag{5}$$

where R is a RV which denotes the dominant scatter position and it is defined at the center of the ellipse in Fig. 2. Finally $\Omega = \{(x, y) \in \mathfrak{R}^2 \mid \sqrt{[x^2 + y^2]} \le R_{BS(MS)}\}$ and $\Omega_{BS(MS)} = \{(x, y) \in \mathfrak{R}^2 \mid \sqrt{[(x \pm F)^2 + y^2]} \le R_{BS(MS)}\}$ where $F^2 = a^2 - b^2$, is the distance from the center of the ellipse to each of its foci.

Now, in order to build the $R_0^{MS(BS)} = R_j^{MS(BS)} - r_j^{MS(BS)}$ PDF, we need to solve the following integral:

$$W_{R_0^{MS(BS)}}(R_0^{MS(BS)}) = \int_{-\infty}^{\infty} W_{r_j^{MS(BS)}}(r_j^{MS(BS)}) W_{R_j^{MS(BS)}}(R_0^{MS(BS)} + r_j^{MS(BS)}) dr_j^{MS(BS)}. \tag{6}$$

The final result is given by:

$$W_{R_0^{MS(BS)}}(R_0^{MS(BS)}) = \frac{2R_0^{MS(BS)} + \frac{4}{3}R_{MS(BS)\min}\delta(R_0^{MS(BS)})}{R^2_{MS(BS)\max} - R^2_{MS(BS)\min}} \tag{7}$$

Even though we have all the PDFs needed for the analysis, we need to refer $W_R(R)$ to the MS and the BS, in order to obtain the $R_0^{MS(BS)}$ PDFs. Note that the azimuth angle must be included in this PDF when referred to the MS or to the BS, and this dependence will have such kind of mirror symmetry around the origin.

4 The Delay and AoA PDF Derivation

In order to make the proper analysis, we will take into account the scenarios that consider up to two reflections in its BS to MS trajectory. According to [Molisch04], those scenarios that consider more than two bounces in their trajectory, contribute with a negligible power to the overall; this is why they can be avoided.

For the macro– and microcell environments (Fig. 1) the possible scenarios are:

1. *Scenario $A_{BS} – B_{BS} – C_{BS} – A_{MS}$.*

2. *Scenario $A_{BS} – C_{MS} – B_{MS} – A_{MS}$.*

3. *Scenario $A_{BS} – B_{BS} – B_{MS} – A_{MS}$.*

4. *Scenario $A_{BS} – B_{BS} – A_{MS}$.*

5. *Scenario $A_{BS} – B_{MS} – A_{MS}$.*

6. *Scenario $A_{BS} – A_{MS}$.*

For the micro– and picocell environment (Fig. 2) the possible scenarios are:

1. *Scenario $A_{BS} – B_{BS} – C – A_{MS}$.*

2. *Scenario $A_{BS} – C – B_{MS} – A_{MS}$.*

3. *Scenario $A_{BS} – B_{BS} – B_{MS} – A_{MS}$.*

    4.   *Scenario $A_{BS} - B_{BS} - A_{MS}$.*

    5.   *Scenario $A_{BS} - B_{MS} - A_{MS}$.*

    6.   *Scenario $A_{BS} - A_{MS}$.*

Note that each scenario from Fig. 1 has its equivalent in Fig. 2, except perhaps by the PDF of the dominant scatter's RV, and because of this, the analysis can be simplified. Furthermore, as scenario 6 both in Fig. 1 and Fig. 2 are completely deterministic with respect to the AoD, AoA and Delay, they will not be considered here. In [Oestges05] it is shown that those scenarios that provide us with more than one bounces with scatters, the MIMO Kronecker model can be properly used.

Here we will use what we call: the transformation's Jacobian [Papoulis02], the direct analytical [Alcocer04] and the mean value [Alcocer05a] approaches in order to get the AOA and Delay PDFs, and depending on the ray tracing scenario and the complexity, it could exist a preference between in their use.

The Transformation Jacobian Approach. Taking into account [Laurila98], in order to obtain the joint Delay and AoA PDF, it is needed to use the PDF transformation rules described in [Papoulis02]. Let us proceed to develop these transformations for some scenarios depicted above:

    4.   *Scenario $A_{BS} - B_{BS} - A_{MS}$.*

In order to find the AoA and Delay statistics, it is needed to find the geometrical relationships such that,

$$\begin{cases} r_j^{BS} = f(c\tau, \varphi_1^{MS}) \\ \theta_1^{BS} = g(c\tau, \varphi_1^{MS}) \end{cases} \tag{8}$$

.

Combining several geometrical relations, we got,

$$r_j^{BS} = \frac{1}{2}\frac{(c\tau)^2 + D^2 - 2(c\tau)D\cos(\varphi_1^{MS})}{(c\tau) - D\cos(\varphi_1^{MS})} \tag{9a}$$

$$\cos(\theta_1^{BS}) = \frac{2(c\tau)D - [(c\tau)^2 + D^2]\cos(\varphi_1^{MS})}{(c\tau)^2 + D^2 - 2(c\tau)D\cos(\varphi_1^{MS})} \tag{9b}$$
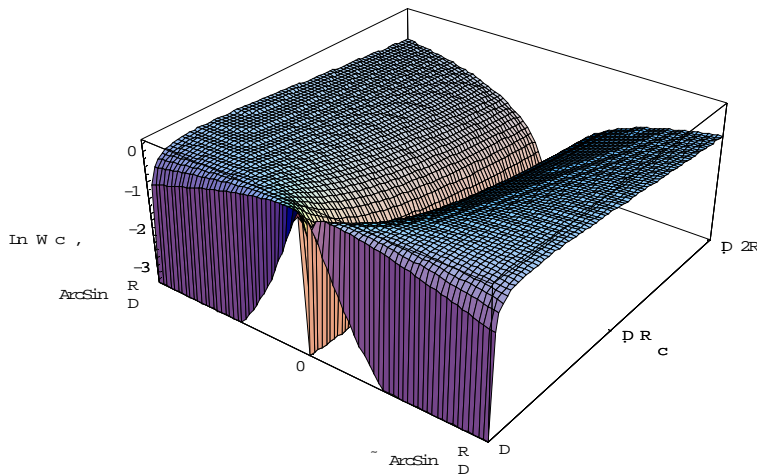

Fig. 3. The joint Delay and AoA PDF for the scenario $A_{BS} - B_{BS} - A_{MS}$.

Finally the joint Delay and AoA PDF is given by,

$$W(c\tau, \varphi_1^{MS}) = \left| J(c\tau, \varphi_1^{MS}) \right| W_{r_j^{BS}}(r_j^{BS}) W_{\theta_1^{BS}}(\theta_1^{BS})$$

$$W(c\tau, \varphi_1^{MS}) = \frac{2}{R_{BS}^2} \frac{(c\tau)^2 + D^2 - 2(c\tau)D\cos(\varphi_1^{MS})}{2(c\tau) - 2D\cos(\varphi_1^{MS})} \cdot \left| \frac{(c\tau)^2 - D^2}{2[(c\tau) - D\cos(\varphi_1^{MS})]^2} \right| W_{\theta_1^{BS}}(\theta_1^{BS}).$$

(10)

A plot of this joint PDF supposing that Wθ(θ1BS) = π–1 sin2 (θ1BS), −π ≤ θ1BS ≤ π, RBS = 30 m and D = 500 m, is given in Fig. 3. Even thought we used typical parameters in the microcell environment, it should be noticed that the PDF depends principally on the RBS/D ratio, the functional form does not change much (see Fig. 3). This will be shown later by the use of the direct analytical approach.

As the marginal AoA PDF can not be seen from the last figure, it is convenient to plot this and it is shown in Fig. 4. The marginal Delay PDF is shown in Fig. 5.
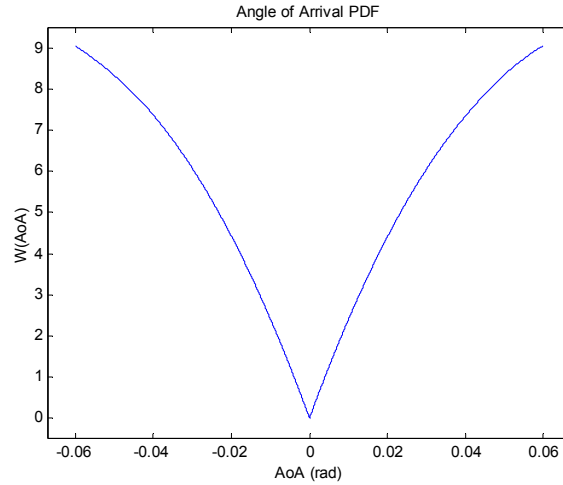

Fig. 4. Marginal AoA PDF.

As it can be seen from Fig. 4, the marginal AoA PDF has a quasi–linear dependence on the AoA RV. This dependence will be shown by the direct analytical approach as well. Fig. 5 shows the ToA or Delay PDF. Note that this plot is scaled to give a best view.
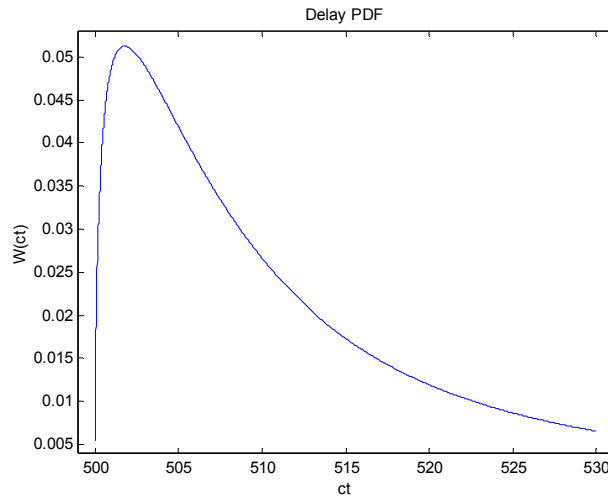

Fig. 5. Marginal Delay PDF.

5. Scenario $A_{BS} - B_{MS} - A_{MS}$.

As well as in scenario 4, it is needed to find the geometrical relationships such that,

$$\begin{cases} r_j^{MS} = f(c\tau, \theta_1^{MS}) \\ \varphi_1^{BS} = g(c\tau, \theta_1^{MS}) \end{cases} \tag{11}$$

Combining several geometrical relations, we got,

$$r_j^{MS} = \frac{1}{2} \frac{(c\tau)^2 + D^2}{(c\tau) - D\cos(\theta_1^{MS})} \tag{12a}$$

$$\tan(\varphi_1^{BS}) = \frac{[(c\tau)^2 - D^2]\sin(\theta_1^{MS})}{2(c\tau)D - [(c\tau)^2 + D^2]\cos(\theta_1^{MS})} \tag{12b}$$

Finally the joint Delay and AoA PDF is given by,

$$W(c\tau, \theta_1^{MS}) = \left| J(c\tau, \theta_1^{MS}) \right| W_{r_j^{MS}}(r_j^{MS}) W_{\varphi_1^{BS}}(\varphi_1^{BS}) \tag{13}$$

$$W(c\tau, \theta_1^{MS}) = \frac{2}{R_{MS}^2} \frac{1}{2} \frac{(c\tau)^2 + D^2}{(c\tau) - D\cos(\theta_1^{MS})} W_{\varphi_1^{BS}}(\varphi_1^{BS}) \cdot \left| \frac{[(c\tau)^2 - D^2][(c\tau)^2 - 2(c\tau)D\cos(\theta_1^{MS}) + D^2\cos(2\theta_1^{MS})]}{2[(c\tau) - D\cos(\theta_1^{MS})]^2[(c\tau)^2 - 2(c\tau)D\cos(\theta_1^{MS}) + D^2]} \right|. \tag{14}$$

A plot of this joint PDF supposing a uniform AoD distribution, $R_{MS} = 30$ m and $D = 500$ m is given in Fig. 6. The joint Delay and AoA PDF for this scenario is in agreement with the one reported in [Ertel99, Fig. 5a], as both of them represent the same communications scenario, i. e., the one with the scatters at the surrounding of the receiver, and they both use a uniform (omni–directional) AoD PDF.
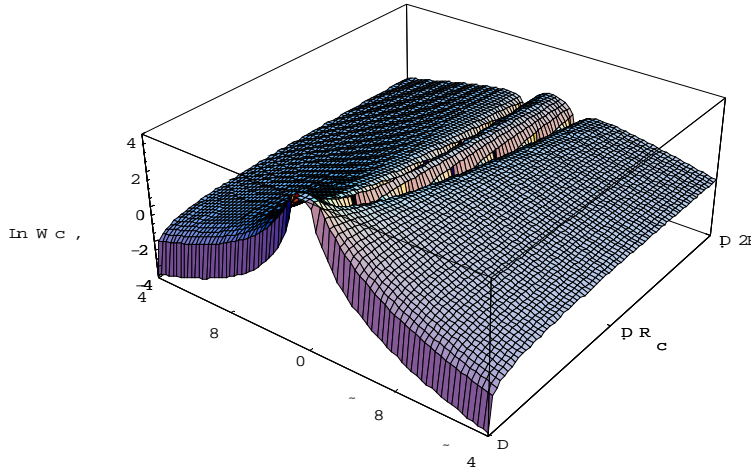
Fig. 6. The joint Delay and AoA for the scenario $A_{BS} - B_{MS} - A_{MS}$.

In Fig. 7, we present the marginal AoA PDF for the case shown in Fig. 6. In Fig. 7 it can be seen that in contrary to Fig. 4, the most probable arrivals are those with low AoA. This behavior can be observed directly from Fig. 6. The marginal Delay PDF is shown in Fig. 8.
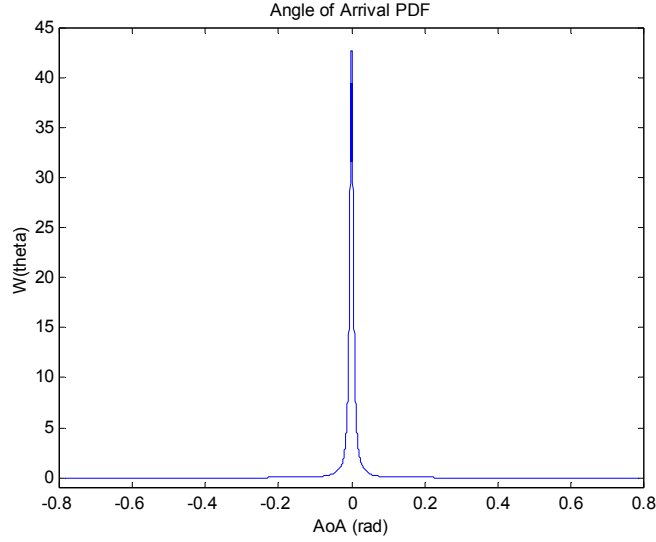
Alberto Alcocer Ochoa, Ramón Parra Michel and Valeri Ya. Kontorovitch

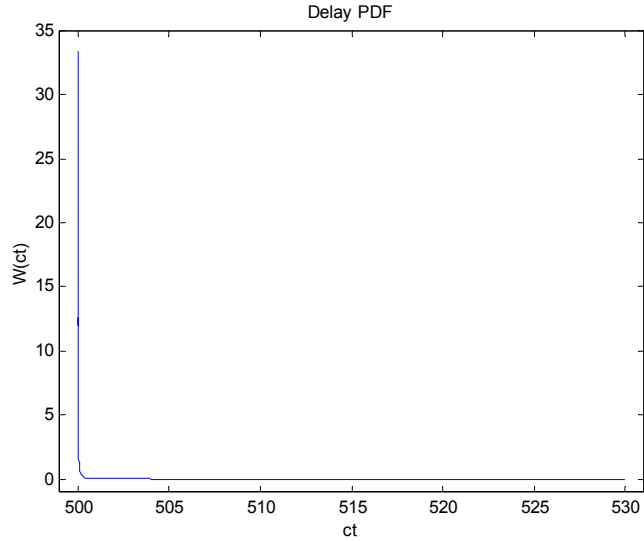**Fig. 7.** Marginal AoA PDF.

Fig. 8. Marginal Delay PDF.

As it can be seen from Fig. 5 and Fig. 8, this approach provides us the marginal Delay PDF, with no more calculus than a simple integral. Furthermore, this approach gives us the exact form of the joint AoA and Delay PDF, as no approximation is used here.

The Direct Analytical Approach. Let us assume the case when D » R(MS)BS,min and DMS(BS) » R0(BS)MS, then the expressions in (1) and (2) can be simplified to,

$$\varphi_1^{MS(BS)} \approx \frac{r_j^{BS(MS)} \sin(\theta_1^{BS(MS)})}{D} \tag{15}$$

$$\varphi_2^{MS(BS)} \approx \frac{R_0^{BS(MS)} \sin(\theta_2^{MS(BS)})}{D_{MS(BS)}} \tag{16}$$

From (15) and (16), and only for those scenarios which have their AoA expressed in terms of $\varphi_1^{MS(BS)}$ and $\varphi_2^{MS(BS)}$, it can be seen that the AoA statistics depends only on the local and dominant scatters region dimension to the MS (BS) separation distance ratio.

334

1. Scenario $A_{BS} - B_{BS} - C_{BS} - A_{MS}$.

Let us consider the expression given in (15) as,

$$\varphi_1^{MS} \approx \frac{r_j^{BS} \sin(\theta_1^{BS})}{D} \tag{17}$$

There are two possible ways to calculate the AoA PDF, and they are:

$$W_{\varphi_1^{MS}}(\varphi_1^{MS}) = \int W_{\varphi_1^{MS}}(\varphi_1^{MS} \mid r_j^{BS}) W_{r_j^{BS}}(r_j^{BS}) dr_j^{BS} \tag{18a}$$

$$W_{\varphi_1^{MS}}(\varphi_1^{MS}) = \int W_{\varphi_1^{MS}}(\varphi_1^{MS} \mid \theta_1^{BS}) W_{\theta_1^{BS}}(\theta_1^{BS}) d\theta_1^{BS} \tag{18b}$$

In [Latinovic04] it is resolved the expression (18a) considering a uniform distribution of the scatters around the BS and a von Mises PDF for the AoD. Here we will consider the other way of calculating the AoA PDF, i. e., using the expression given in (18b). Again, by using (17) we got,

$$W_{\varphi_1^{MS}}(\varphi_1^{MS} \mid \theta_1^{BS}) = W_{r_j^{BS}}\left(\frac{D\varphi_1^{MS}}{\sin(\theta_1^{BS})}\right)\left|\frac{D}{\sin(\theta_1^{BS})}\right| \tag{19}$$

$$W_{\varphi_1^{MS}}(\varphi_1^{MS} \mid \theta_1^{BS}) = \frac{2D^2}{\sin^2(\theta_1^{BS})} \frac{\varphi_1^{MS}}{R_{BS,min}^2} \tag{20}$$

Finally, the AoA PDF is given by,

$$W_{\varphi_1^{MS}}(\varphi_1^{MS}) = \frac{2D^2\varphi_1^{MS}}{R_{BS,min}^2} \int \frac{W_{\theta_1^{BS}}(\theta_1^{BS})}{\sin^2(\theta_1^{BS})} d\theta_1^{BS} \tag{21}$$

$$W_{\varphi_1^{MS}}(\varphi_1^{MS}) = \frac{2D^2\left|\varphi_1^{MS}\right|}{R_{BS,min}^2}\left\langle \csc^2(\theta_1^{BS})\right\rangle_{\theta_1^{BS}}, \quad \left|\varphi_1^{MS}\right| \leq \frac{R_{BS,min}}{D} \tag{22}$$

As it can be seen, the last expression has a linear dependence on the variable φ1MS, as it is approximately shown in Fig. 4. The absolute value in (22) is only a merely mathematical formalism as Fig. 3 and Fig. 4 suggest it.

Let us explain that besides the fact that both formulas (18a) and (18b) give formally the same result Wφ(φ1MS), actually they belong to different communication scenarios.

The first one belongs to the following concept: let us suppose that in any mental experiment (realization) of the communications downlink, the angle θ1BS is randomly given by Wθ(θ1BS), and thanks to this randomness, the angle φ1MS is random as well; the distance rjBS is random with Wr(rjBS) but fixed during each experiment realization. Another experiment will deal with another random value of rjBS. By averaging all the experiments[1] one gets Wφ(φ1MS) (Fig. 9).

The second scenario for the calculus of Wφ(φ1MS) deals with the assumption that the random angle θ1BS is fixed during the experiment and due to the random nature of rjBS, the angle φ1MS is random as well. Another experiment will deal with another random value of θ1BS. Again by averaging all the experiments one can get Wφ(φ1MS) (Fig. 10).

---

[1] By *averaging all the experiments*, we mean averaging the results for the set of different communication links with the above mentioned assumptions due to $W_\theta(\theta_1^{BS})$ and $W_r(r_j^{BS})$.
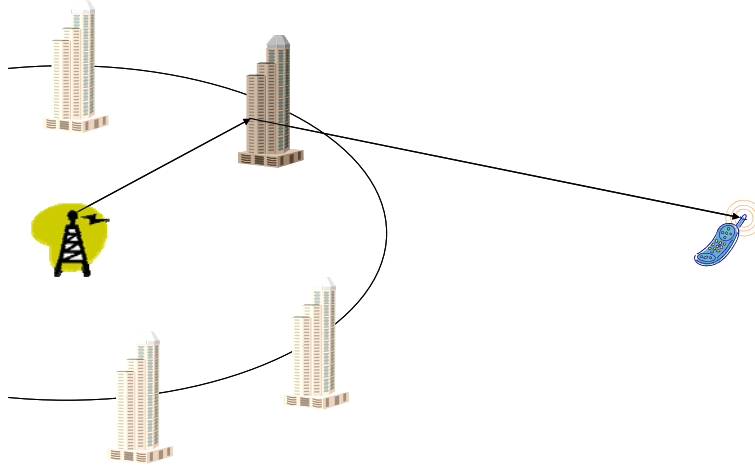
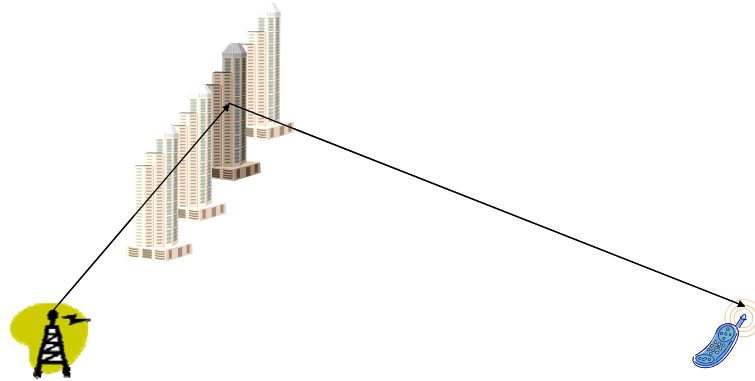**Fig. 9.** Scenario modeled by expression (18a).

Fig. 10. Scenario modeled by expression (18b).

One can easily see that those scenarios are completely different due to the non–linearity of the functional dependence of φ1MS from θ1BS, and the linear dependence of φ1MS from rjBS. For this matter, the operations for functional transform and averaging are not commutative, so the final functional forms for Wφ(φ1MS) will differ for both scenarios.

It is worth to mention that the first scenario refers to the well know Jakes' model [Jakes79] and actually is valid for omni–directional antennas at both sides of the transmission link. In contrary, the second scenario assumes a high grade of directionality for illumination (random for different experiments) of the scatters volume, and actually the receiving antenna is only gathering the energy dispersed form the scatters, while at the first scenario the receiving energy is formed by certain scatters which are able to reflect part of the energy radiated, e. g., uniformly. Actually the second scenario is realistic for macro– and picocell environments, due to the fast motion of the scatters during the communications link.

The assumption of the von Mises distribution in [Latinovic04] does not change the concept, because the angle φ1MS for D » RBS,min is very small. In order to finish with the analysis of this scenario it is necessary to consider (16) as,

$$\varphi_2^{MS} \approx \frac{R_0^{BS}\sin(\theta_2^{BS})}{D_{MS}} \tag{23}$$

Again (see (18a) and (18b)), there are two possible ways to calculate the PDF for this angle, and they are,

$$W_{\varphi_2^{MS}}(\varphi_2^{MS}) = \int W_{\varphi_2^{MS}}(\varphi_2^{MS} \mid R_0^{BS})W_{R_0^{BS}}(R_0^{BS})dR_0^{BS} \tag{24a}$$

$$W_{\varphi_2^{MS}}(\varphi_2^{MS}) = \int W_{\varphi_2^{MS}}(\varphi_2^{MS} \mid \theta_2^{BS})W_{\theta_2^{BS}}(\theta_2^{BS})d\theta_2^{BS} \tag{24b}$$

Here we will resolve this case by using the expression given in (24b). The final result is given in (25),

$$W_{\phi_2^{MS}}(\phi_2^{MS}) = \frac{2D^2\phi_2^{MS}}{R_{BS,max}^2 - R_{BS,min}^2}\left\langle csc^2(\theta_2^{BS})\right\rangle_{\theta_2^{BS}} + \frac{4}{3}\frac{R_{BS,min}\delta(\phi_2^{MS})}{R_{BS,max}^2 - R_{BS,min}^2}, \quad \left|\phi_2^{MS}\right| \le \frac{R_{BS,min}}{2D_{MS}}. \tag{25}$$

Then, as the AoA is given by $\phi^{MS} = \phi_1^{MS} + \phi_2^{MS}$, as in expression (26), finally the AoA PDF for this scenario 1, in the macrocell environment is given by (27).

$$W_{\phi^{MS}}(\phi^{MS}) = \left\langle csc^2(\theta_1^{BS})\right\rangle_{\theta_1^{BS}}\left\langle csc^2(\theta_2^{BS})\right\rangle_{\theta_2^{BS}} \cdot \int_{\frac{R_{BS,min}}{2D_{MS}}}^{\frac{R_{BS,max}}{2D_{MS}}} \frac{2D^2(\phi - \phi_2^{MS})}{R_{Bs,min}^2}\frac{2D_{MS}^2\phi_2^{MS}}{R_{Bs,max}^2 - R_{Bs,min}^2}d\phi_2^{MS}, \tag{26}$$

$$W_{\phi^{MS}}(\phi^{MS}) = \left\langle csc^2(\theta_1^{BS})\right\rangle_{\theta_1^{BS}}\left\langle csc^2(\theta_2^{BS})\right\rangle_{\theta_2^{BS}} \cdot \frac{4D2}{3}\left[\frac{3\phi^{MS} - \frac{R_{BS,max}}{D_{MS}}}{R_{BS,min}^2} - \frac{1}{D_{MS}}\frac{\delta(\phi^{MS})}{R_{BS,max} + R_{BS,min}}\right], \quad 0 \le \phi^{MS} - \frac{R_{BS,max}}{3D_{MS}} \le \frac{R_{BS,min}}{2D_{MS}}.$$

$$\dots (27)$$

4. Scenario $A_{BS} - B_{BS} - A_{MS}$.

Due to the equivalency to the solution in the scenario 1, here we will need only the expression (22), which proposes a quasi–linear behavior of the AoA PDF, as stated above, and this can be seen directly from Fig. 4.

As it was stated before, in (22) and (27) it can be seen the linear dependence of the AoA PDF. This behavior is shown in Fig. 4 as well, and will be shown later by the use of the mean value approach.

The Mean Value Approach. Let us consider expression (17) and the mean value of the scatters' position RV at the BS, rjBS which is denoted as rm = <rjBS> = 2 RBS,min / 3, and the final result is given by,

$$W_{\phi_1^{MS}}(\phi_1^{MS}) = \frac{2D^3(\phi_1^{MS})^2}{\pi r_m^2\sqrt{r_m^2 - D^2(\phi_1^{MS})^2}}, \quad \left|\phi_1^{MS}\right| \le \frac{r_m}{D} \tag{28}$$

In Fig. 11, it is shown the AoA PDF using the same values as in Fig. 3 and Fig. 4. As it can be seen form Fig. 11, the quasi–linear behavior of the AoA PDF is valid only under a limited region around the origin. Note that the same phenomenon is shown in Fig. 4, by using the transformation's Jacobian approach.
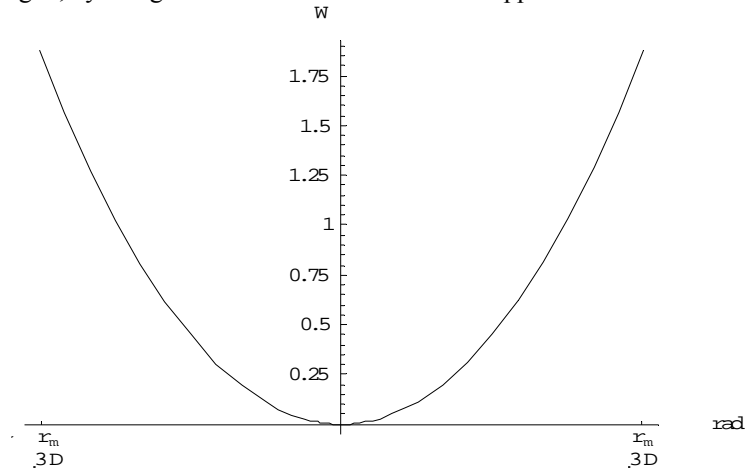

Fig. 11. The AoA PDF obtained using the Mean Value Approach.

Even though the exact form of the AoA PDF is given by the transformation's Jacobian approach, for more complex scenarios, i. e. for those that consider two bounces, the algebra complicates too much and in those cases the other approaches can be used.

5 Conclusions

As it was shown in the AoA PDF plots, the behavior of the normalized PAS are quite similar no matter the environment used, as long as the distance between the MS and the BS being greater than the scatters region sizes, i. e., as the ratio RMS(BS),min / D remains low.

Here we showed three different approaches in order to solve the problem of geometrical modeling of the channel, even though we only used them in a few scenarios, we believe they can be proposed to solve the others. Their used would depend on the information we need to obtain as the complexity arises as more information is required.

The results obtained here would allow us to derive a closed PDP expression for the calculation of the spatial covariation matrix element. This is done in order to apply an orthogonalization approach for its representation and proper simulation.

In [Alcocer05b] the authors are presenting some basic properties of the spatial covariation matrix for the MIMO channel, using the results obtained from the use of the geometrical model presented here. The results obtained by this allow us to propose the prolate spheroidal wave functions (PSWF) as a good candidate set for the spatial domain channel expansion.

Here it is shown the results for the AoA or in a more general sense the PAS, and as it can be seen from [SCM03] (as an example), several geometrical standards agree with these results. The same apply with the ToA statistics, which are in accordance with those shown at the COST 207 standard.

References

1. [Alcocer04] A. Alcocer–Ochoa, R. Parra–Michel & V. Kontorovitch. "Wideband MIMO Channel Based on Geometrical Approximations". I International Conference on Electric and Electronic Engineering and X Conference on Electrical Engineering 2004, ICEEE–CIE 2004, September 8–10, 2004. Acapulco, Guerrero, México.
2. [Alcocer05a] A. Alcocer–Ochoa, R. Parra–Michel & V. Kontorovitch. "The Elliptical Geometrical Channel Model for the Micro– and Picocell Environments in Wideband MIMO Communications Systems". 6th World Wireless Congress 2005, WWC 2005. 24–27 May, Palo Alto, California, U.S.A.
3. [Alcocer05b] A. Alcocer–Ochoa, R. Parra–Michel & V. Kontorovitch. "Some General Properties of the Covariation Matrix for MIMO Communications Channels". Fourth Generation Mobile Forum 2005, 4GMF 2005, 11–13 July San Diego, California, U.S.A.
4. [Chen04] Y. Chen & V. K. Dubey. "Accuracy of Geometric Channel–Modeling Methods". IEEE Transactions on Vehicular Technology. Vol. 53, No. 1, Pages 82–93, January 2004.
5. [Chizhik02] D. Chizhik, G. J. Foshini, M. J. Gans & R. A. Valenzuela. "Keyholes, Correlations and Capacities of Multi–element Transmit and Receive Antennas". IEEE Transactions on Wireless Communications. Vol. 1, No. 2, Pages 361–368, April 2002.
6. [Ertel98] R. B. Ertel, P. Cardieri, K. W. Sowerby, T. S. Rappaport & J. H. Reed. "Overview of Spatial Channel Models for Antenna Array Communication Systems". IEEE Personal Communications. Pages 10–22, February 1998.
7. [Ertel99] R. B. Ertel & J. H. Reed. "Angle and Time of Arrival Statistics for Circular and Elliptical Scattering Models". IEEE Journal on Selected Areas in Communications. Vol. 17, No. 11, Pages 1829–1840, November 1999.
8. [Jakes79] W. C. Jakes. "Microwave Mobile Communications". *John Wiley & Sons*, New York, 1979.
9. [Kontorovitch99] V. Kontorovitch, R. Linares & H. Jardón. "Theoretical Approach Applied to EMC Measurement Problems". International Journal of Modeling and Simulation. Vol. 19, No. 4, Pages 384–389, 1999.
10. [Latinovic04] Z. Latinovic, A. Abdi & Y. Bar–Ness. "On the Utility of the Circular Ring Model for Wideband Channels". IEEE Transactions on Vehicular Technology Conference, VTC 2004 Fall, September 2004, Los Angeles, Ca. U.S.A.
11. [Laurila98] J. Laurila, A. F. Molisch & E. Bonek. "Influence of the Scatters Distribution on the Power Delay Profile and the Power Azimuth Spectra of Mobile Radio Channels". IEEE Proceedings of the 5th International Symposium on Spread Spectrum Techniques and Applications 1998. Vol. 1, Pages 267–271, September 2–4, 1998.
12. [Molisch04] A. F. Molisch. "A Generic Model for MIMO Wireless Propagation Channels in Macro– and Microcells". IEEE Transactions on Signal Processing. Vol. 52, No. 1, Pages 61–71, January 2004.
13. [Oestges03] C. Oestges, V. Erceg & A. J. Paulraj. "A Physical Scattering Model for MIMO Macrocellular Broadband Wireless Channels". IEEE Journal on Selected Areas in Communications. Vol. 21, No. 5, Pages 721–729, June 2003.
14. [Oestges05] C. Oestges, B. Clerckx, D. Vanhoenacker–Janvier & A. J Paulraj. "Impact of Fading Correlations on MIMO Communication Systems in Geometry–Based Statistical Channel Models". IEEE Transactions on Wireless Communications, Vol. 4, No. 3. Pages 1112–1120. May 2005.
15. [Papoulis02] A. Papoulis & S. U. Pillai. "Probability, Ramdom Variables, and Stochastic Processes". McGraw Hill. 4th Edition, New York, 2002.

16. [Piechocki01] R. J. Piechocki, J. P. McGeehan & G. V. Tsoulus. "A New Stochastic Spatio–Temporal Propagation Model (SSTPM) for Mobile Communications with Antenna Arrays". IEEE Transactions on Communications. Vol. 49, No. 5, Pages 855–862, May 2001.
17. [SCM03] SCM. "Spatial Channel Model Text Description". Spatial Channel Model AHG (Combined ad–hoc form 3GPP & 3GPP2), April 2003.

Alberto Alcocer Ochoa *was born in the city of Puebla, Mexico in 1977. He received the B. Sc. degree in Physics and Mathematics from the National Polytechnic Institute of Mexico in 2000 and the M. Sc. degree in Electrical Engineering from the CINVESTAV–IPN in 2003. Currently, he is studying at CINVESTAV–IPN, towards his Ph. D. degree in Electrical Engineering. His main research interest includes radio propagation modeling and digital signal processing.*

Ramon Parra Michel *was born in Guadalajara city, Mexico, in 1973. He received the B. Sc. degree in Electronics and Communications form the University of Guadalajara in 1996 and the M. Sc. and Ph. D. degree in Electrical Engineering from the CINVESTAV–IPN in 1998 and 2003 respectively. Currently, he is working at CINVESTAV–IPN. His research interest includes modeling and simulation of radio channels and digital communication system design.*

Valeri Kontorovitch *was born in Sverdlovsk, Russia in 1941. He received the B. E. E. and M. S. E. E. degrees in 1963, the Ph. D. degree in 1968, and the D. Sc. degree in radio communication systems in 1986, all from the State University of Telecommunications (St. Pt. UT). Since 1993 he has been with the CINVESTAV–IPN in Mexico. His present interests are in Dynamic System Theory, modeling of communication channels and interference.*